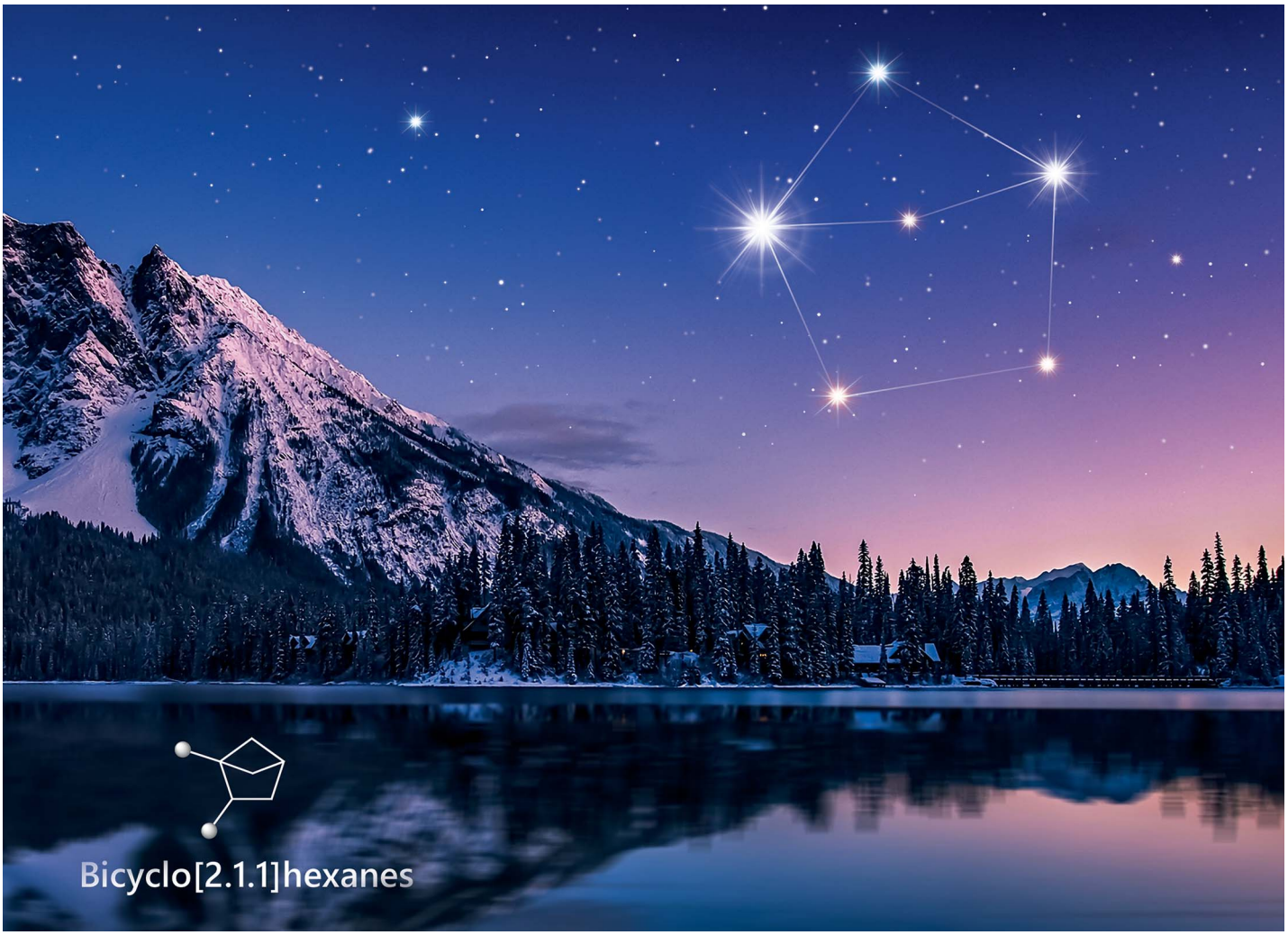

Showcasing research from Professor Mykhailiuk's laboratory, Enamine, Kyiv, Ukraine.

1,2-Disubstituted bicyclo[2.1.1]hexanes as saturated bioisosteres of *ortho*-substituted benzene

The cover picture shows a constellation of the 1,2-disubstituted bicyclo[2.1.1]hexane scaffold – a saturated bioisostere of the *ortho*-substituted benzene. This scaffold has been developed and studied by Mykhailiuk and coworkers at Enamine (Ukraine, Kyiv).

As featured in:

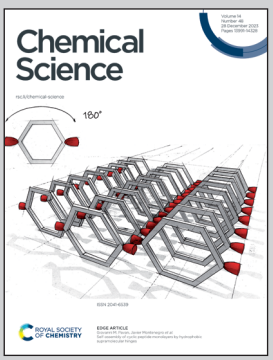

See Pavel K. Mykhailiuk *et al.*, *Chem. Sci.*, 2023, **14**, 14092.

ROYAL SOCIETY OF CHEMISTRY

rsc.li/chemical-science

Registered charity number: 207890

Chemical Science

ROYAL SOCIETY OF CHEMISTRY

EDGE ARTICLE

View Article Online
View Journal | View Issue

Check for updates

Cite this: *Chem. Sci.*, 2023, **14**, 14092

All publication charges for this article have been paid for by the Royal Society of Chemistry

Received 28th September 2023
Accepted 25th October 2023

DOI: 10.1039/d3sc05121h

rsc.li/chemical-science

Open Access Article. Published on 27 ottobre 2023. Downloaded on 12/02/2026 06:37:49.
This article is licensed under a Creative Commons Attribution 3.0 Unported Licence.

1,2-Disubstituted bicyclo[2.1.1]hexanes as saturated bioisosteres of *ortho*-substituted benzene†

Aleksandr Denisenko,[a] Pavel Garbuz,[a] Yelyzaveta Makovetska,[a] Oleh Shablykin,[ab] Dmytro Lesyk,[c] Galeb Al-Maali,[ad] Rodion Korzh,[a] Iryna V. Sadkova[a] and Pavel K. Mykhailiuk *[a]

Bicyclo[2.1.1]hexanes have been synthesized, characterized, and biologically validated as saturated bioisosteres of the *ortho*-substituted benzene ring. The incorporation of the 1,2-disubstituted bicyclo[2.1.1]hexane core into the structure of fungicides boscalid (BASF), bixafen (Bayer CS), and fluxapyroxad (BASF) gave saturated patent-free analogs with high antifungal activity.

Introduction

The benzene ring is a basic structural unit in chemistry, and we learn about it in school. It is the most popular ring in natural products[1] and bioactive compounds.[2,3]

The *ortho*-substituted benzene ring, in particular, is found in the structure of more than three hundred drugs and agrochemicals (Fig. 1).[4,5] For example, the well-known drug aspirin contains an *ortho*-substituted benzene ring. Recently, we discovered that 1,5-disubstituted bicyclo[2.1.1]hexanes and their oxa-containing analogs can mimic the *ortho*-substituted benzene ring in bioactive compounds (Fig. 1).[6] These scaffolds were synthesized as a mixture of two diastereomers. Some of them were subsequently separated by crystallization or column chromatography. In many cases, however, the separation of diastereomers failed, and the desired products were not obtained.

Pleasingly, these studies were well received by the scientific community, and the groups of Glorius,[7] Brown,[8] Procter,[9] Li,[10] Wang,[11] and Studer[12] subsequently developed alternative approaches to di- and poly-substituted bicyclo[2.1.1]hexanes based on the functionalization of bicyclo[1.1.0]butanes.[13–15]

In this work, we have synthesized, characterized, and biologically validated 1,2-disubstituted bicyclo[2.1.1]hexanes as a new generation of saturated bioisosteres of *ortho*-substituted benzenes. These structural cores exist as single diastereomers. Bicyclo[2.1.1]hexanes were incorporated into the structure of fungicides boscalid (BASF), bixafen (Bayer CS), and

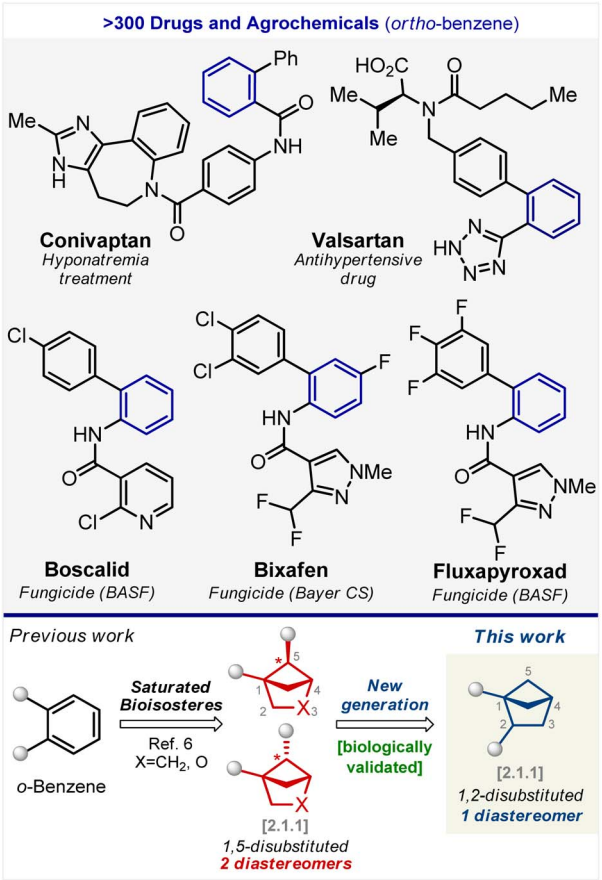

Fig. 1 Bicyclo[2.1.1]hexanes as saturated bioisosteres of the *ortho*-substituted benzene ring: state of the art.

[a]*Enamine Ltd, Winston Churchill st. 78, 02094 Kyiv, Ukraine; Web: www.mykhailiukchem.org. E-mail: Pavel.Mykhailiuk@gmail.com*

[b]*V. P. Kukhar Institute of Bioorganic Chemistry and Petrochemistry of the NAS of Ukraine, 02094 Kyiv, Ukraine*

[c]*Bienta, Winston Churchill st. 78, 02094 Kyiv, Ukraine*

[d]*Institute of Botany of the National Academy of Sciences of Ukraine, 02094 Kyiv, Ukraine*

† Electronic supplementary information (ESI) available. CCDC 2286521 and 2286523–2286527. For ESI and crystallographic data in CIF or other electronic format see DOI: https://doi.org/10.1039/d3sc05121h

© 2023 The Author(s). Published by the Royal Society of Chemistry

Open Access Article. Published on 27 ottobre 2023. Downloaded on 12/02/2026 06:37:49.
This article is licensed under a Creative Commons Attribution 3.0 Unported Licence.

fluxapyroxad (BASF) to provide saturated patent-free analogs with high antifungal activity.

Results and discussion

Design

Benzene (C_6H_6; M.W. = 78) is an aromatic molecule. Among the conformationally rigid bi(poly)cyclic saturated scaffolds, – bicyclo[1.1.1]pentane,[16] bicyclo[3.1.1]heptane,[17] cubane,[18] and bicyclo[2.1.1]hexane (Fig. 2), – only the latter has the same number of carbon atoms and a similar molecular weight (C_6H_{10}; M.W. = 82; Fig. 2b).[19,20] Three types of substitution patterns in bicyclo[2.1.1]pentane can potentially mimic the *ortho*-benzene ring geometry: 1,2-, 1,5-, and 2.3- (Fig. 2b). While two latter cores exist as two diastereomers, the 1,2-disubstituted bicyclo[2.1.1]pentanes exist as only one diastereomer (Fig. 2). Moreover, this scaffold was recently proposed to mimic the *ortho*-substituted benzene ring; however, biological validation of this hypothesis was not made.[9] In this work, we report a practical approach to 1,2-disubstituted bicyclo[2.1.1]hexanes and show with biological experiments that this core indeed can act as a bioisostere of the *ortho*-substituted benzene ring in bioactive compounds.

Synthesis

Despite numerous studies on the topic,[7–15] we needed a practical approach to bicyclo[2.1.1]hexanes with only two substituents (two exit vectors) at the 1- and 2-positions of the core (Scheme 1) without additional (poly)substitution at other positions. Moreover, one substituent should be (hetero)aromatic, and another one should be the carboxylic group, which is needed for the subsequent modifications of the core *via* amide coupling.[21,22]

In light of our previous experience,[6] we wondered if diene **1** (easily obtained from acetophenone, please see Scheme 1) would undergo an intramolecular photocycloaddition into the desired bicyclo[2.1.1]hexane core. Direct irradiation of diene **1** in acetonitrile at different wavelengths gave only traces of products (entries 1–4, Table 1). Irradiation with a broad wavelength mercury lamp gave the target product in 35% yield along with the formation of unidentified side products (entry 5). We also tried available organic ketones for the triplet sensitization of the styrene moiety. Cleaner formation of the desired bicyclo[2.1.1]hexane **1a** was observed (entries 6–10). The best yield of 76% was obtained with benzophenone (entry 8), whereas thioxanthone also worked well (entry 7). Among all tested solvents (entries 11–14), the best result was obtained in acetonitrile. Without irradiation, the reaction did not take place (entry 15).

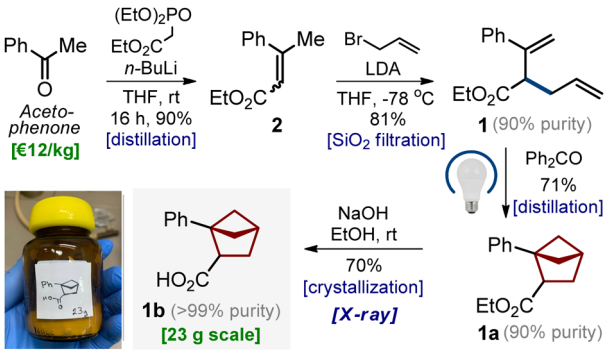

Scheme 1 Gram-scale synthesis of bicyclo[2.1.1]hexane **1b** from acetophenone.

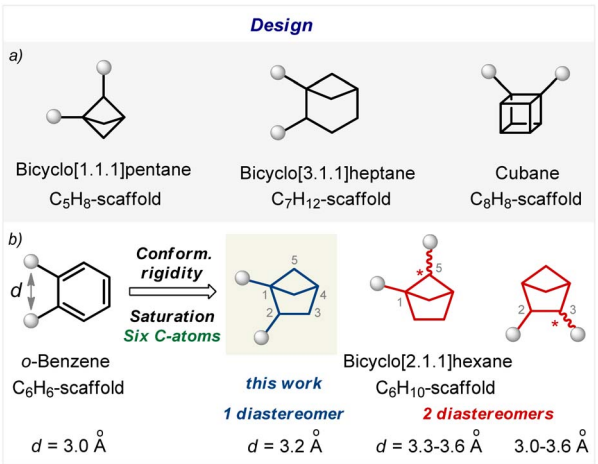

Fig. 2 Design of saturated bioisosteres of the *ortho*-substituted benzenes. (a) Disubstituted bicyclo[1.1.1]pentanes, bicyclo[3.1.1] heptanes, and cubanes. (b) Disubstituted bicyclo[2.1.1]hexanes.

Table 1 Optimization of the synthesis of bicyclo[2.1.1]hexane **1a**

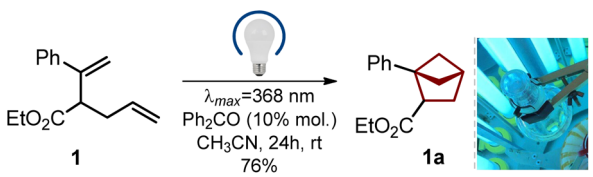

Entry	Conditions	Yield[a,b] (%)
1	450 nm, CH_3CN	n.r.
2	368 nm, CH_3CN	<10
3	313 nm, CH_3CN	<10
4	254 nm, CH_3CN	<20
5	Broad wavelength Hg lamp, CH_3CN	35
6	368 nm, CH_3CN, acetophenone	43
7	368 nm, CH_3CN, thioxanthone	54
8	368 nm, CH_3CN, benzophenone	(82)76[c]
9	368 nm, CH_3CN, $(p\text{-}NO_2C_6H_4)_2CO$	31
10	368 nm, CH_3CN, $(p\text{-}Me0C_6H_4)_2CO$	62
11	368 nm, CH_2Cl_2 Ph_2CO	47
12	368 nm, Me_2CO, Ph_2CO	45
13	368 nm, PhMe, Ph_2CO	31
14	368 nm, EtOAc, Ph_2CO	43
15	In the dark, rt	n.r.

[a] 100 mmol scale. [b] ^1H NMR yield (CH_2Br_2 as an internal standard). [c] Isolated yield after column chromatography. See the ESI for details. n.r.: no reaction.

Open Access Article. Published on 27 ottobre 2023. Downloaded on 12/02/2026 06:37:49.
This article is licensed under a Creative Commons Attribution 3.0 Unported Licence.

Scalable synthesis

The entire optimized synthetic protocol is shown in Scheme 1. It was important for us to elaborate on a modular method that would provide bicyclo[2.1.1]hexanes employing only available and inexpensive starting materials. The synthesis started from acetophenone. The Horner–Wadsworth–Emmons reaction of acetophenone smoothly gave alkene **2** in 90% yield after distillation. Treatment of the latter with LDA in THF at −78 °C followed by the addition of allyl bromide gave diene **1** in 81% yield (*ca.* 90% purity). The compound contained *ca.* 10% of the isomeric diene, as the undesired alkylation at the methyl group also took place (please see the ESI,† p. S5–S6). An analytically pure sample of diene **1** was obtained by purification with HPLC. In the next step, however, we used the crude material. An intramolecular photocycloaddition of diene **1** proceeded smoothly on scale to provide the desired bicyclo[2.1.1]hexane **1a** in 71% yield (*ca.* 90% purity) after distillation. Saponification of the ester group in **1a** followed by crystallization from hexane–*t*BuOMe gave pure carboxylic acid **1b** as a white crystalline solid in 70% yield. The structure of compound **1b** was confirmed by X-ray crystallographic analysis (Scheme 2).[23]

It is important to note that following this optimized sequence, we easily synthesized 23 g of product **1b** in one run. No column chromatography was involved at any step.

Scope

We studied the scope of the developed method. The photochemical reaction tolerated various substituents at the aromatic core (Scheme 2). Among them were an alkyl group (**7**); fluorine (**4**, **14**, and **15**), chlorine (**5** and **13**) and bromine atoms (**6** and **11**); methoxy (**9** and **10**) and trifluoromethyl groups (**8** and **12**). All three substitution patterns of the benzene ring, – *para* (**4**–**10**), *meta* (**11**–**14**), and *ortho* (**15**), – gave the corresponding bicyclo[2.1.1]hexanes **4a**–**15a** in 67–73% yield. The photocycloaddition was also compatible with the fluorine atom directly attached to the diene structure (**3** and **10**). Various medicinal chemistry-relevant heterocycles, such as pyrazole (**16** and **17**), imidazole (**18**), thiophene (**19**), furane (**20**), and pyridine (**21**–**23**), provided the desired bicyclo[2.1.1]hexanes **16a**–**23a** in 57–76% yield. All products **3a**–**23a** were purified by distillation. Saponification of the ester group in **3a**–**23a** followed by crystallization gave solid carboxylic acids **3b**–**23b** in 63–76% yield.

All final products were synthesized in gram quantities. The structures of bicyclo[2.1.1]hexanes **1b**, **3b**, **4b**, **10b**, and **12b** were confirmed by X-ray crystallographic analysis (Scheme 2).[23]

Modifications

Compounds **1b** and **3b**–**23b** possess one functional group (–CO_2H). We aimed to perform some representative modifications of these bicyclo[2.1.1]hexanes to obtain linkers for medicinal chemistry – compounds with two functional groups.

Esterification of carboxylic acid **1b**, followed by oxidation of the phenyl group with $NaIO_4$/$RuCl_3$ gave linker **24** (Scheme 2). The fluorine-substituted linker **25** was synthesized analogously from compound **3b**. Both linkers **24** and **25** provide a way to synthesize various 1,2-disubstituted bicyclo[2.1.1]hexanes by standard stepwise modifications of carboxylic groups (amide synthesis, heterocyclizations, radical couplings, *etc.*).[24]

Crystallographic analysis

Next, we compared the geometric parameters of 1,2-disubstituted bicyclo[2.1.1]hexanes with those of the *ortho*-substituted benzene ring. For this, we employed the exit vector plot tool. In this method, two substituents on the scaffold were simulated by two exit vectors n_1 and n_2 (Fig. 3). The relative spatial arrangement of the vectors is described by four geometric parameters: the distance between C-atoms r, the plane angles φ_1 (between vectors n_1 and C–C) and φ_2 (between vectors n_2 and C–C), and the dihedral angle θ defined by vectors n_1, C–C and n_2. An additional representative parameter – the distance d between two carbon substituents (Fig. 3) – was also measured.

We calculated the values of d, r, φ_1, φ_2, and /θ/of 1,2-disubstituted bicyclo[2.1.1]hexanes from the X-ray data of compounds **1b**, **4b**, and **12b**.[23]

The corresponding parameters for *ortho*-substituted benzene were obtained from the reported crystal data of two antihypertensive drugs – valsartan and telmisartan (Fig. 3).[25] Analysis of these data revealed that the geometric properties of 1,2-disubstituted bicyclo[2.1.1]hexanes in general were similar to those of *ortho*-substituted benzene. In particular, the distance d in bicyclo[2.1.1]hexanes was only 0.1 Å longer than that in the *ortho*-benzene ring: 3.05–3.19 Å (**1b**, **4b**, and **12b**) *vs.* 3.04–3.10 Å (*ortho*-benzene).

The distance r in bicyclo[2.1.1]hexane was *ca.* 0.1–0.2 Å longer than that in the *ortho*-benzene ring: 1.56 Å (**1b**, **4b**, and **12b**) *vs.* 1.39–1.41 Å (*ortho*-benzene).

Angles φ_1 and φ_2 were similar in both scaffolds: 61–65° (**1b**, **4b**, and **12b**) *vs.* 55–57° (*ortho*-benzene). The difference in planarity, however, between the saturated scaffold and the benzene ring was significant: while *ortho*-benzene was almost flattened, bicyclo[2.1.1]hexanes had a significant three-dimensional character:/θ/= 56–59° (**1b**, **4b**, and **12b**) *vs.* 7–8° (*ortho*-benzene).

In general, both distances r and d and angles φ_1 and φ_2 of 1,2-disubstituted bicyclo[2.1.1]hexanes were similar to those of the *ortho*-substituted benzene ring.

Incorporation into bioactive compounds

The incorporation of the bicyclo[2.1.1]hexane scaffold into bioactive compounds was then attempted. We chose five drugs and agrochemicals with an *ortho*-substituted benzene ring: agent for hyponatremia treatment conivaptan, lipid-lowering agent lomitapide (Scheme 3); fungicides boscalid, bixafen, and fluxapyroxad (Scheme 4).

Synthesis of the saturated analog of conivaptan was performed from carboxylic acid **1b** (Scheme 3). Amide coupling with the corresponding *para*-substituted aniline gave the desired compound **26**. Compound **27**, – a saturated analog of lomitapide, – was obtained analogously from carboxylic acid **8b** (Scheme 3).

© 2023 The Author(s). Published by the Royal Society of Chemistry

Open Access Article. Published on 27 ottobre 2023. Downloaded on 12/02/2026 06:37:49.
This article is licensed under a Creative Commons Attribution 3.0 Unported Licence.

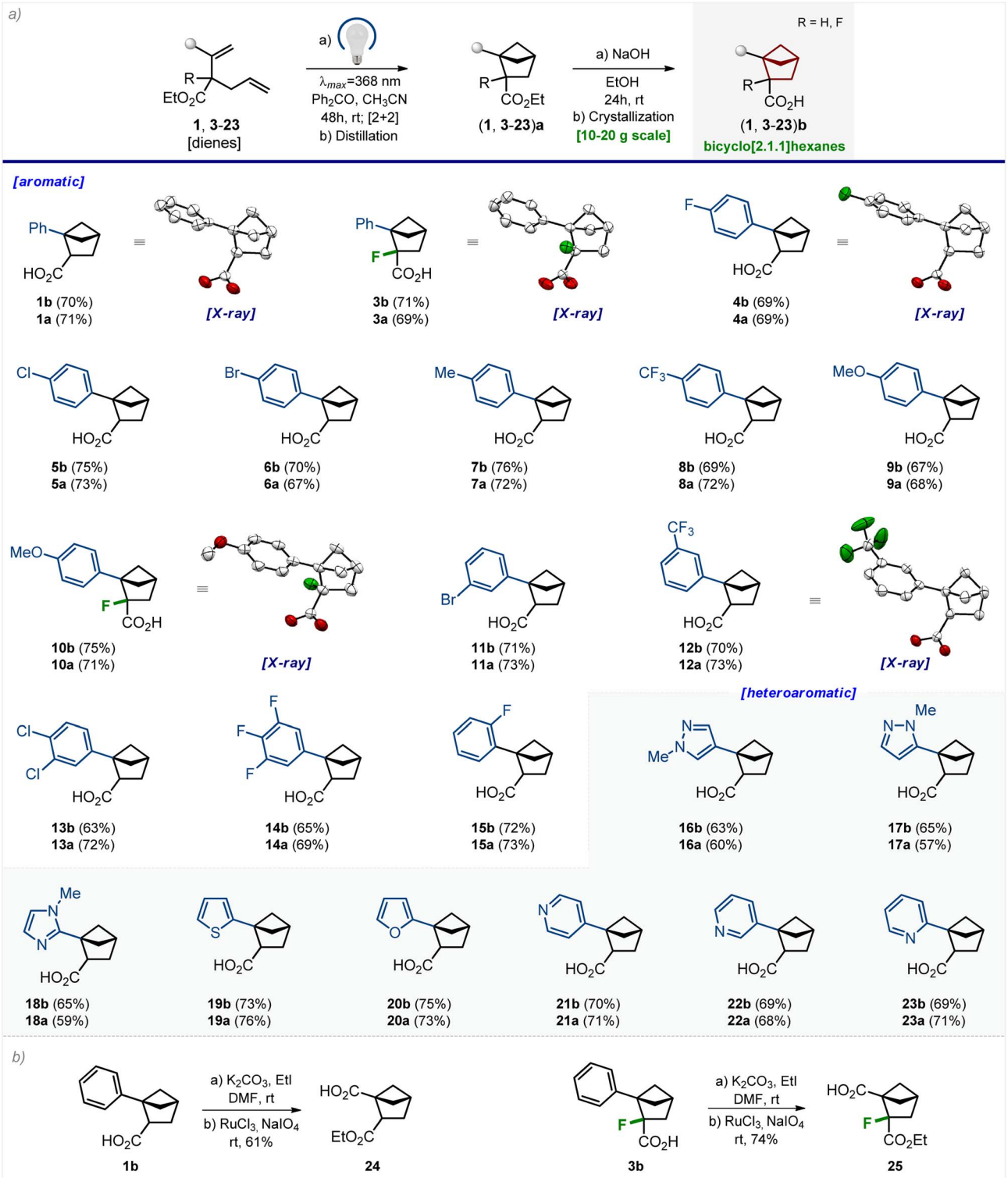

Scheme 2 (a) Scope of the reaction. X-ray crystal structure of compounds **1b**, **3b**, **4b**, **10b**, and **12b** (carbon – white, oxygen – red, and fluorine – green). Hydrogen and chlorine atoms are omitted for clarity. Ellipsoids are shown at a 50% probability level. (b) Synthesis of linkers **24** and **25**.

Synthesis of the saturated analog of boscalid was performed from carboxylic acid **5b** (Scheme 4). The Curtius reaction followed by acylation of the intermediate amine with 2-chloropyridine-3-carboxylic acid gave compound **28.** Using an analogous strategy, compound **29,** – a saturated analog of bixafen, – was obtained from carboxylic acid **13b** (Scheme 4). The saturated analog of fluxapyroxad, compound **30,** was synthesized from carboxylic acid **14b.**

Open Access Article. Published on 27 ottobre 2023. Downloaded on 12/02/2026 06:37:49.
This article is licensed under a Creative Commons Attribution 3.0 Unported Licence.

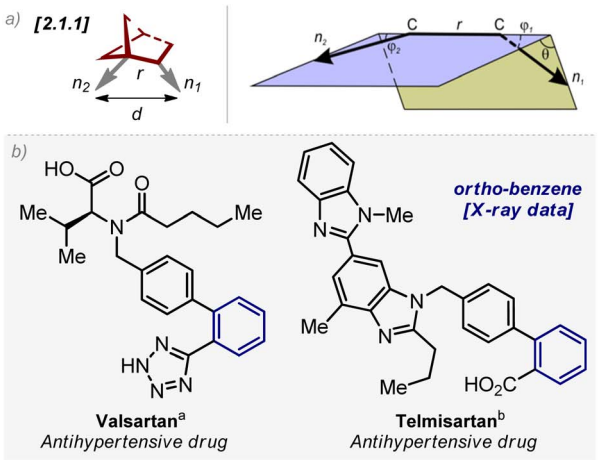

Compound	d (Å)	r (Å)	φ_1 (°)	φ_2 (°)	$\lvert\theta\rvert$ (°)
Valsartan	3.036(2)	1.414(2)	56.6(1)	56.9(1)	8.3(2)
Telmisartan	3.101(7)	1.385(7)[c]	55.3(5)	55.2(5)	7.5(8)
1b	3.190(4)	1.557(3)	65.1(2)	61.3(2)	58.6(3)
4b	3.178(3)	1.560(3)	64.9(2)	62.2(2)	58.8(2)
12b	3.048(3)	1.557(3)	69.0(2)	64.0(2)	55.5(3)

Fig. 3 (a) Definition of vectors n_1 and n_2, and geometric parameters d, r, φ_1, φ_2 and θ. 1,2-Disubstituted bicyclo[2.1.1]hexane is shown as an example. (b) Geometric parameters d, r, φ_1, φ_2, and $|\theta|$ for *ortho*-substituted benzenes (*valsartan* and *telmisartan*); and bicyclo[2.1.1]hexanes **1b**, **4b**, and **12b**. [a]Data are taken from ref. 25a. [b]Data are taken from ref. 25b. [c]Two molecules of telmisartan are present in the crystalline lattice with $r = 1.385(7)$Å and 1.395(7)Å (ref. 25b).

The structures of bicyclo[2.1.1]hexanes **28** and **29** were confirmed by X-ray crystallographic analysis.[23]

Physicochemical parameters

We studied the effect of the replacement of the *ortho*-substituted benzene ring by bicyclo[2.1.1]hexanes on the physicochemical properties of bioactive compounds (Schemes 3 and 4).

Water solubility. Replacement of the *ortho*-benzene ring in conivaptan by bicyclo[2.1.1]hexane (**26**) increased the solubility by threefold: 5 μM (conivaptan) *vs.* 14 μM (**26**) (Scheme 3). An analogous trend was observed with lomitapide. Replacement of the benzene ring in lomitapide with bicyclo[2.1.1]hexane (**27**) led to a dramatic sixfold increase in solubility: 3 μM (lomitapide) *vs.* 18 μM (**27**).

Replacement of the *ortho*-benzene ring by bicyclo[2.1.1]hexane in agrochemicals boscalid, bixafen, and fluxapyroxad produced conflicting results. In boscalid, such a replacement led to a significant threefold increase in solubility: 11 μM (boscalid) *vs.* 35 μM (**28**). In bixafen, the opposite effect was observed, and the solubility was reduced: 30 μM (bixafen) *vs.* 4 μM (**29**).[26] In fluxapyroxad, such a replacement resulted in a slight increase in solubility: 25 μM (fluxapyroxad) *vs.* 27 μM (**30**).

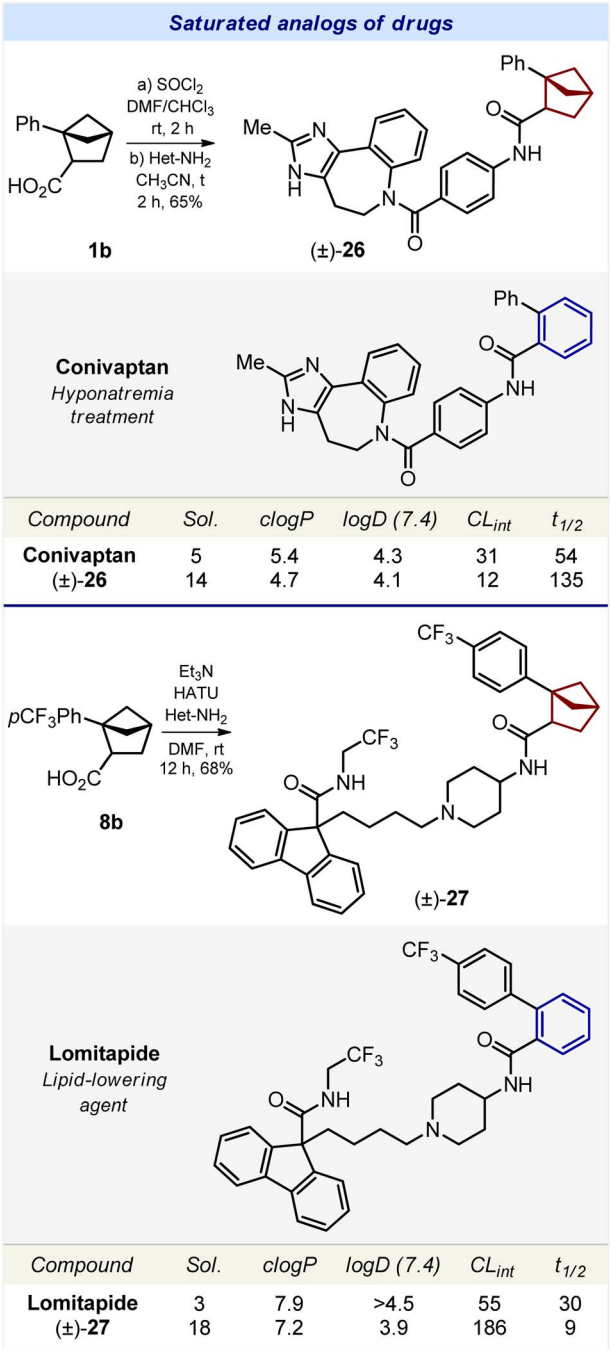

Compound	Sol.	clogP	logD (7.4)	CL_{int}	$t_{1/2}$
Conivaptan	5	5.4	4.3	31	54
(±)-**26**	14	4.7	4.1	12	135

Compound	Sol.	clogP	logD (7.4)	CL_{int}	$t_{1/2}$
Lomitapide	3	7.9	>4.5	55	30
(±)-**27**	18	7.2	3.9	186	9

Scheme 3 Synthesis and properties of compounds **26** and **27** – saturated analogs of drugs conivaptan and lomitapide, correspondingly. HATU: hexafluorophosphate azabenzotriazole tetramethyl uronium. Sol.: the experimental kinetic solubility in phosphate-buffered saline, pH 7.4 (μM). *c* log *P*: the calculated lipophilicity. log *D* (7.4): the experimental distribution coefficient in *n*-octanol/phosphate-buffered saline, pH 7.4. Reliable log *D* values could be obtained within a range of 1.0–4.5. CL_{int}: the experimental metabolic stability in human liver microsomes (μL min^{-1} mg^{-1}). $t_{1/2}$ (min): the experimental half-time of metabolic decomposition.

© 2023 The Author(s). Published by the Royal Society of Chemistry

Open Access Article. Published on 27 ottobre 2023. Downloaded on 12/02/2026 06:37:49.
This article is licensed under a Creative Commons Attribution 3.0 Unported Licence.

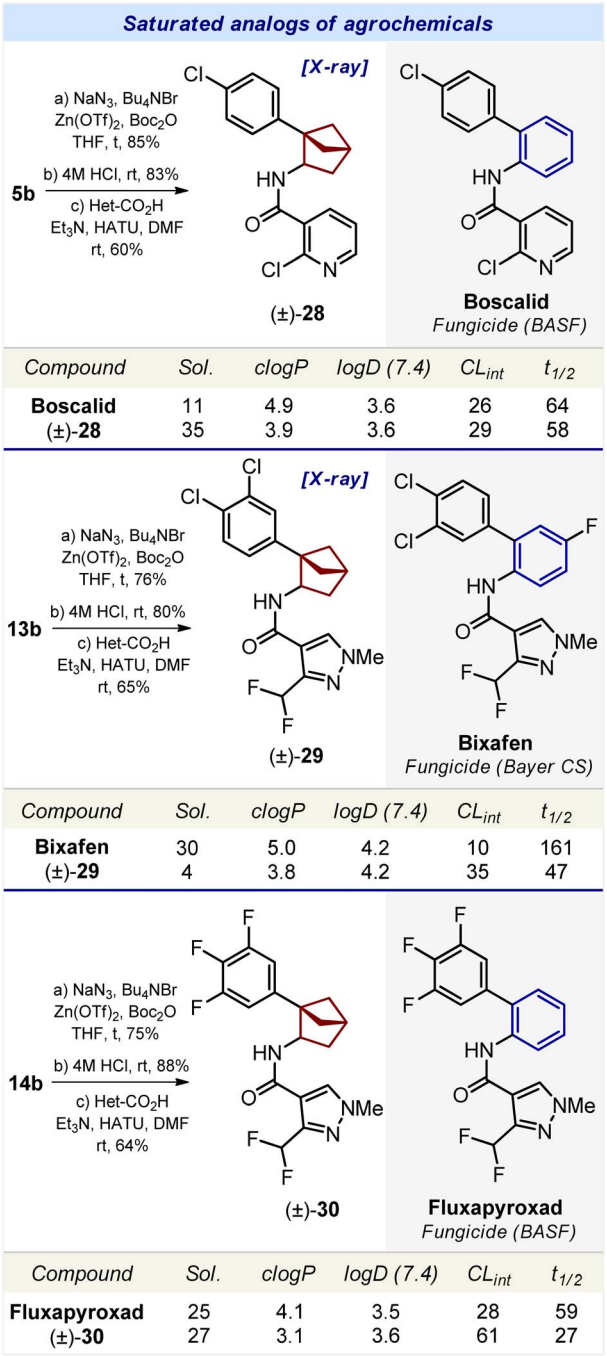

Compound	Sol.	clogP	logD (7.4)	CL_{int}	$t_{1/2}$
Boscalid	11	4.9	3.6	26	64
(±)-**28**	35	3.9	3.6	29	58

Compound	Sol.	clogP	logD (7.4)	CL_{int}	$t_{1/2}$
Bixafen	30	5.0	4.2	10	161
(±)-**29**	4	3.8	4.2	35	47

Compound	Sol.	clogP	logD (7.4)	CL_{int}	$t_{1/2}$
Fluxapyroxad	25	4.1	3.5	28	59
(±)-**30**	27	3.1	3.6	61	27

Scheme 4 Synthesis and properties of compounds **28–30** – saturated analogs of agrochemicals boscalid, bixafen, and fluxapyroxad, correspondingly. Sol.: the experimental kinetic solubility in phosphate-buffered saline, pH 7.4 (μM). *c* log *P*: the calculated lipophilicity. log *D* (7.4): the experimental distribution coefficient in *n*-octanol/phosphate-buffered saline, pH 7.4. Reliable log *D* values could be obtained within a range of 1.0–4.5. CL_{int}, clearance intrinsic (μL min^{-1} mg^{-1}): experimental metabolic stability in human liver microsomes. $t_{1/2}$ (min): the experimental half-time of metabolic decomposition.

In conclusion, in four out of the five bioactive compounds, the replacement of the *ortho*-benzene ring by bicyclo[2.1.1]hexane led to an enhanced water solubility.

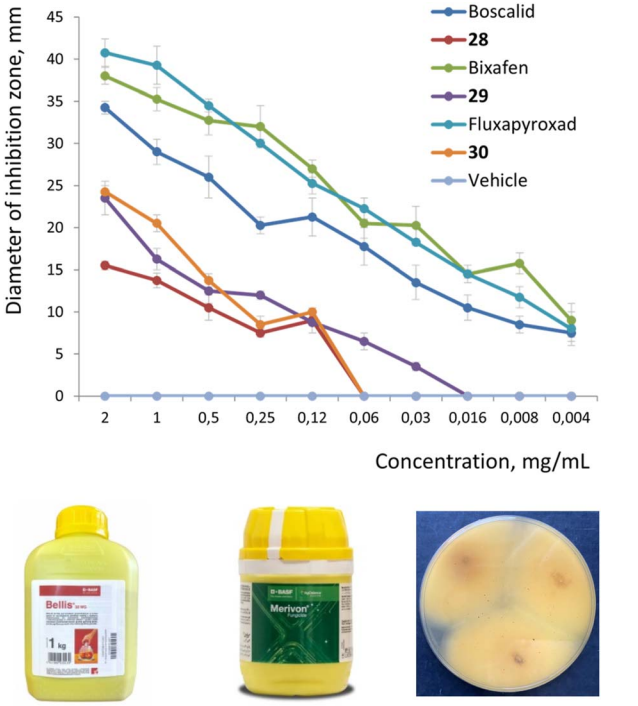

Fig. 4 Inhibition of growth of *Aspergillus niger* (strain VURV-F 822; measured as a diameter of the inhibition zone, mm) with boscalid, bixafen, fluxapyroxad, and their analogs **28–30** at different concentrations after 48 h of incubation. Fungicides boscalid (@Bellis) and bixafen (@Merivon) are shown. Inhibition of fungal growth by compound **29**.

Lipophilicity. To estimate the influence of the replacement of the *ortho*-benzene ring with bicyclo[2.1.1]hexane on lipophilicity, we used two parameters: calculated lipophilicity (*c* log *P*)[27] and experimental lipophilicity (log *D*).

Replacement of the *ortho*-benzene ring in conivaptan, lomitapide, boscalid, bixafen, and fluxapyroxad with bicyclo[2.1.1]hexane (**26–30**) led to a decrease in *c* log *P* by 0.7–1.2 units.

Replacement of the *ortho*-benzene ring with bicyclo[2.1.1]hexane had only a small effect on the logD index. In four bioactive compounds (conivaptan, boscalid, bixafen, and fluxapyroxad) such a replacement almost did not affect log *D*. Only in lomitapide, the saturated analog **27** had a significantly lower log *D* index: >4.5 (lomitapide) *vs.* 3.9 μM (**27**).

In summary, in all five bioactive compounds, replacement of the *ortho*-benzene ring by bicyclo[2.1.1]hexane led to a decrease in calculated lipophilicity (*c* log *P*) by 0.7–1.2 units; and in four of them it had little effect on the experimental lipophilicity (log *D*).

Metabolic stability. The effect of bicyclo[2.1.1]hexane on the metabolic stability of bioactive compounds was more complex. In conivaptan, the incorporation of bicyclo[2.1.1]hexane (**26**) increased the metabolic stability: CL_{int} (μL min^{-1} mg^{-1}) = 31 (conivaptan) *vs.* 12 (**26**). In lomitapide, bixafen, and fluxapyroxad the incorporation of bicyclo[2.1.1]hexane (**27**, **29**, and **30**) dramatically decreased the metabolic stability by two (**30**) to three (**27**, **29**) times, as measured by using $t_{1/2}$ (min). In

Open Access Article. Published on 27 ottobre 2023. Downloaded on 12/02/2026 06:37:49. This article is licensed under a Creative Commons Attribution 3.0 Unported Licence.

boscalid, such a replacement led to a slight decrease in metabolic stability: CL_{int} (μL min^{-1} mg^{-1}) = 26 (boscalid) *vs.* 29 (**28**) (Schemes 3 and 4).

In brief summary, in four out of the five bioactive compounds, replacement of the *ortho*-benzene ring with bicyclo[2.1.1]hexane decreased the metabolic stability.

Bioactivity

Finally, we wanted to answer the key question, – can 1,2-disubstituted bicyclo[2.1.1]hexanes indeed act as bioisosteres of the *ortho*-benzene ring in bioactive compounds?[9] Therefore, we measured the antifungal activity of the marketed fungicides boscalid (BASF), bixafen (Bayer CS), fluxapyroxad (BASF), and their saturated analogs **28–30**. In strict contrast to medicinal chemistry, the use of racemic mixtures in agrochemistry is common;[5] therefore for the validation of the proof-of-concept, we directly studied the biological activity of the available racemic compounds **28–30** (Fig. 4).

We measured the antifungal activity of all six compounds against the fungal strain *Aspergillus niger*, – using the disk diffusion method (ESI, p. S327–S333†). Even though the original agrochemicals were more potent, all three saturated analogs **28–30** were active and showed a high inhibition of the growth of *Aspergillus niger* compared to the vehicle (Fig. 4; and ESI, p. S327–S333†).

Conclusions

In this work, we have synthesized, characterized, and biologically validated 1,2-disubstituted bicyclo[2.1.1]hexanes as saturated bioisosteres of the *ortho*-substituted benzenes. These structures were obtained from readily available and inexpensive starting materials (acetophenone) on a multigram scale (Schemes 1 and 2). Physicochemical and geometric properties of bicyclo[2.1.1]hexanes were measured and compared to those of the *ortho*-substituted benzenes (Fig. 3). The incorporation of the bicyclo[2.1.1]hexane core into the structure of agrochemicals boscalid (BASF), bixafen (Bayer CS), and fluxapyroxad (BASF) gave the saturated patent-free analogs **28–30** with high antifungal activity.

We believe that given the commonplace of the phenyl group in chemistry, its saturated bioisosteres developed here will become common in medicinal chemistry in the coming years.

Data availability

The ESI† contains method description, product characterization data, and NMR spectra.

Author contributions

A. D. and P. K. M. designed the project. A. D., P. G., Y. M., O. S., G. A.-M., and R. K. carried out the experiments. I. V. S. and P. K. M. wrote the manuscript and all authors provided comments.

Conflicts of interest

A. D., P. G., Y. M., O. S., G. A.-M., R. K., I. V. S., and P. K. M. are employees of a chemical supplier Enamine.

Acknowledgements

The authors are grateful to Prof. A. A. Tolmachev for the support of this work. This project has received funding from the European Research Council (ERC) under the European Union's Horizon 2020 research and innovation program (grant agreement no. 101000893 – BENOVELTY). PM is very grateful to Dr S. Shishkina (IOC, Kyiv) for the X-ray studies; to Dr P. Borysko (Bienta), Dr Y. Holota (Bienta), and Mrs L. Bortnichuk (Bienta) for ADME studies; to Dr Vladimir Kubyshkin (Enamine) and Dr Bill Heilman for proofreading the text and helpful suggestions.

Notes and references

1 Y. Chen, C. Rosenkranz, S. Hirte and J. Kirchmair, *Nat. Prod. Rep.*, 2022, **39**, 1544–1556.
2 R. D. Taylor, M. MacCoss and A. D. G. Lawson, *J. Med. Chem.*, 2014, **57**, 5845–5859.
3 J. Shearer, J. L. Castro, A. D. G. Lawson, M. MacCoss and R. D. Taylor, *J. Med. Chem.*, 2022, **65**, 8699–8712.
4 **www.drugbank.ca**.
5 *The Pesticide Manual*, ed. C. MacBean, British Crop Production Council, 2012.
6 (*a*) A. Denisenko, P. Garbuz, N. M. Voloshchuk, Y. Holota, G. Al-Maali, P. Borysko and P. K. Mykhailiuk, *Nat. Chem.*, 2023, **15**, 1155–1163; (*b*) A. Denisenko, P. Garbuz, S. V. Shishkina, N. M. Voloshchuk and P. K. Mykhailiuk, *Angew. Chem., Int. Ed.*, 2020, **59**, 20515–20521.
7 (*a*) R. Kleinmans, T. Pinkert, S. Dutta, T. O. Paulisch, H. Keum, C. G. Daniliuc and F. Glorius, *Nature*, 2022, **605**, 477–482; (*b*) R. Kleinmans, S. Dutta, K. Ozols, H. Shao, F. Schafer, R. E. Thielemann, H. T. Chan, C. G. Daniliuc, K. N. Houk and F. Glorius, *J. Am. Chem. Soc.*, 2023, **145**, 12324–12332.
8 R. Guo, Y.-C. Chang, L. Herter, C. Salome, S. E. Braley, T. Fessard and M. K. Brown, *J. Am. Chem. Soc.*, 2022, **144**, 7988–7994.
9 S. Agasti, F. Beltran, E. Pye, N. Kaltsoyannis, G. E. M. Crisenza and D. J. Procter, *Nat. Chem.*, 2023, **15**, 535–541.
10 M. Xu, Z. Wang, Z. Sun, Y. Ouyang, Z. Ding, T. Yu, L. Xu and P. Li, *Angew. Chem., Int. Ed.*, 2022, **61**, e202214507.
11 Y. Liu, S. Lin, Y. Li, J.-H. Xue, Q. Li and H. Wang, *ACS Catal.*, 2023, **13**, 5096–5103.
12 N. Radhoff, C. G. Daniliuc and A. Studer, *Angew. Chem., Int. Ed.*, 2023, **62**, e202304771.
13 New photochemical approaches to bicyclo[2.1.1]hexanes appeared recently: (*a*) L. Herter, I. Koutsopetras, L. Turelli, T. Fessard and C. Salomé, *Org. Biomol. Chem.*, 2022, **20**, 9108–9111; (*b*) T. Rigotti and T. Bach, *Org. Lett.*, 2022, **24**, 8821–8825; (*c*) S. Paul, D. Adelfinsky, C. Salome, T. Fessard and M. K. Brown, *Chem. Sci.*, 2023, **14**, 8070–8075; (*d*)

© 2023 The Author(s). Published by the Royal Society of Chemistry

Open Access Article. Published on 27 ottobre 2023. Downloaded on 12/02/2026 06:37:49. This article is licensed under a Creative Commons Attribution 3.0 Unported Licence.

M. Reinhold, J. Steinebach, C. Golza and J. C. L. Walker, *Chem. Sci.*, 2023, **14**, 9885–9891; (*e*) R. Jeyaseelan, M. Utikal, C. G. Daniliuc and L. Næsborg, *Chem. Sci.*, 2023, **14**, 11040–11044.

14 For the synthesis of bicyclo[2.1.1]hexane-containing boronates, see: Y. Yang, J. Tsien, J. M. E. Hughes, B. K. Peters, R. R. Merchant and T. Qin, *Nat. Chem.*, 2021, **13**, 950–955.

15 2-Oxabicyclo[2.1.1]hexanes: (*a*) Y. Liang, R. Kleinmans, C. G. Daniliuc and F. Glorius, *J. Am. Chem. Soc.*, 2022, **144**, 20207–20213; (*b*) Y. Liang, F. Paulus, C. G. Daniliuc and F. Glorius, *Angew. Chem., Int. Ed.*, 2023, **62**, e202305043.

16 (*a*) X. Ma, Y. Han and D. J. Bennett, *Org. Lett.*, 2020, **22**, 9133–9138; (*b*) J.-X. Zhao, Y.-X. Chang, C. He, B. J. Burke, M. R. Collins, M. D. Bel, J. Elleraas, G. M. Gallego, T. P. Montgomery, J. J. Mousseau, S. K. Nair, M. A. Perry, J. E. Spangler, J. C. Vantourout and P. S. Baran, *Proc. Natl. Acad. Sci. U.S.A.*, 2020, **118**, e2108881118; (*c*) O. L. Garry, M. Heilmann, J. Chen, Y. Liang, X. Zhang, X. Ma, C. S. Yeung, D. J. Bennett and D. W. C. MacMillan, *J. Am. Chem. Soc.*, 2023, **145**, 3092–3100; (*d*) B. A. Wright, A. Matviitsuk, M. J. Black, P. García-Reynaga, L. E. Hanna, A. T. Herrmann, M. K. Ameriks, R. Sarpong and T. P. Lebold, *J. Am. Chem. Soc.*, 2023, **145**, 10960–10966.

17 (*a*) A. S. Harmata, T. E. Spiller, M. J. Sowden and C. R. J. Stephenson, *J. Am. Chem. Soc.*, 2021, **143**, 21223–21228; (*b*) N. Frank, J. Nugent, B. R. Shire, H. D. Pickford, P. Rabe, A. J. Sterling, T. Zarganes-Tzitzikas, T. Grimes, A. L. Thompson, R. C. Smith, C. J. Schofield, P. E. Brennan, F. Duarte and E. A. Anderson, *Nature*, 2022, **611**, 721–726; (*c*) T. Iida, J. Kanazawa, T. Matsunaga, K. Miyamoto, K. Hirano and M. Uchiyama, *J. Am. Chem. Soc.*, 2022, **144**, 21848–21852; (*d*) Y. Zheng, W. Huang, R. K. Dhungana, A. Granados, S. Keess, M. Makvandi and G. A. Molander, *J. Am. Chem. Soc.*, 2022, **144**, 23685–23690; (*e*) T. Yu, J. Yang, Z. Wang, Z. Ding, M. Xu, J. Wen, L. Xu and P. Li, *J. Am. Chem. Soc.*, 2023, **145**, 4304–4310.

18 (*a*) B. A. Chalmers, H. Xing, S. Houston, C. Clark, S. Ghassabian, A. Kuo, B. Cao, A. Reitsma, C.-E. P. Murray, J. E. Stok, G. M. Boyle, C. J. Pierce, S. W. Littler, D. A. Winkler, P. V. Bernhardt, C. Pasay, J. J. De Voss, J. McCarthy, P. G. Parsons, M. T. Smith, H. M. Cooper, S. K. Nilsson, J. Tsanaktsidis, G. P. Savage and C. M. Williams, *Angew. Chem., Int. Ed.*, 2016, **55**, 3580–3585; (*b*) M. P. Wiesenfeldt, J. A. Rossi-Ashton, I. B. Perry, J. Diesel, O. L. Garry, F. Bartels, S. C. Coote, X. Ma, C. S. Yeung, D. J. Bennett and D. W. C. MacMillan, *Nature*, 2023, **618**, 513–518; (*c*) T. A. Reekie, C. M. Williams, L. M. Rendina and M. Kassiou, *J. Med. Chem.*, 2019, **62**, 1078–1095.

19 P. M. Mykhailiuk, *Org. Biomol. Chem.*, 2019, **17**, 2839–2849.

20 M. A. M. Subbaiah and N. A. Meanwell, *J. Med. Chem.*, 2021, **64**, 14046–14128.

21 The most popular reaction in medicinal chemistry is the synthesis of amides from carboxylic acids and amines: D. G. Brown and J. Boström, *J. Med. Chem.*, 2016, **59**, 4443–4458.

22 Amines could be easily obtained from carboxylic acids via the Curtius reaction (see the ESI, p. S45–S48).†

23 Cambridge Crystallographic Data Center (CCDC) deposition numbers: **1b** (2286523), **3b** (2286521), **4b** (2286526), **10b** (2286525), **12b** (2286524), **31** (2286523) and **32** (2286527).

24 This tactic is currently being used to obtain 1,3-disubstituted bicyclo[1.1.1]pentanes by the stepwise modifications of the carboxylic groups in bicyclo[1.1.1]pentane-1,3-dicarboxylic acid: V. Ripenko, D. Vysochyn, I. Klymov, S. Zhersh and P. K. Mykhailiuk, *J. Org. Chem.*, 2021, **86**, 14061–14068.

25 (*a*) J.-R. Wang, X. Wang, L. Lu and X. Mei, *Cryst. Growth Des.*, 2013, **13**, 3261–3269; (*b*) R. Chadha, S. Bhandari, J. Haneef, S. Khullar and S. Mandal, *CrystEngComm*, 2014, **16**, 8375–8389.

26 Technically, the comparison of bixafen and its saturated analog **29** is not accurate, because bixafen has an additional polar C(sp^2)–F bond, and analog **29** does not have it.

27 *c* log *P* was calculated with ChemAxon Marvin Sketch (version 22.13).

© 2023 The Author(s). Published by the Royal Society of Chemistry